Obliquely Propagating Dust-Density Plasma Waves in the Presence of an Ion Beam

A. Piel,* M. Klindworth, and O. Arp
IEAP, Christian-Albrechts-Universität zu Kiel, D-24098 Kiel, Germany

A. Melzer and M. Wolter
Institut für Physik, Ernst-Moritz-Arndt-Universität Greifswald, D-17489 Greifswald, Germany
(Received 24 August 2006; published 17 November 2006)

Self-excited dust-density waves are experimentally studied in a dusty plasma under microgravity. Two types of waves are observed: a mode inside the dust volume propagating in the direction of the ion flow and a new mode propagating obliquely at the boundary between the dusty plasma and the space-charge sheath. A model for dust-density waves propagating at an arbitrary angle with respect to the ion-flow direction is presented, which explains the preference for oblique or parallel modes as a function of ion velocity.

DOI: 10.1103/PhysRevLett.97.205009 PACS numbers: 52.27.Lw, 52.35.Fp, 52.35.Qz

Introduction.—Dust-density waves (DDWs) were observed as a self-excited mode in many dusty plasma experiments, e.g., [1–6]. The DDWs resemble the dust-acoustic wave (DAW) [7] but are also affected by ion drift effects. The theory of ion-dust streaming instabilities in collisional plasmas, such as processing plasmas, was discussed by various authors [8–12]. On the other hand, the excitation of DAWs in magnetized collisionless plasmas, by cross-field currents, is of interest for planetary ring plasmas. Bharuthram [13] showed that DAWs can become unstable in the ring system of Saturn, when a wide regime of propagation angles around the perpendicular direction is considered. In this Letter we report on the observation of a new kind of obliquely propagating dust-density waves (OPDDWs), which are quite unusual in an unmagnetized dusty plasma, and give an explanation of this phenomenon in terms of a linear instability analysis.

The experiments were performed in a 13.56 MHz radio-frequency (rf) parallel plate discharge under microgravity during the 7th DLR (German Aerospace Center) parabolic flight campaign (2005). A vertical cross section through the center of the presently used IMPF-K device is sketched in Fig. 1. The original IMPF (International Microgravity Plasma Facility) device was described in Ref. [14]. In IMPF-K, the electrodes now consist of a central disk and two concentric rings. The rf discharge is operated with two independent rf power generators that feed the disk and the ring electrodes in a push-pull mode. The axial gap between the electrodes is 30 mm wide and the outer ring has a diameter of 80 mm. The IMPF-K device is equipped with the two-dimensionally scanning Langmuir probe system for measuring the plasma parameters described in Ref. [14]. The rf discharge is operated in argon at pressures of 15–50 Pa. Typical rf voltages are $U_{\mathrm{rf}} = 50$–$100 V_{\mathrm{pp}}$. We use monodisperse melamine particles of radius $a = 3.4\ \mu$m. Typical plasma conditions are: ion density $n_i \approx 1 \times 10^{15}\ \mathrm{m}^{-3}$ and electron temperature $T_e = 2.5$–4 eV.

DDWs are observed with a vertically expanded sheet of laser light and a fast digital camera with a usable field of view of $60 \times 30\ \mathrm{mm}^2$ as indicated in Fig. 1. The corresponding camera resolution is 1280×640 pixels. The frame rate was chosen as 100 fps to avoid any aliasing of wave signals, which have frequencies of $f \approx 10$ Hz.

Experimental observations.—Self-excited DDWs are observed at low gas pressure and high dust density. The following results were obtained at $p = 15$ Pa and $U^d_{\mathrm{rf}} = 65 V_{\mathrm{pp}}$. Inner and outer ring were electrically connected and operated at $U^r_{\mathrm{rf}} = 55 V_{\mathrm{pp}}$. A typical still image, which represents a central section through the dust cloud, is shown in Fig. 2. The dust distribution shows the formation of a central dust-free region (''void''), an oval ring of dust and a dark dust-free space-charge sheath in front of both electrodes. The boundary of the dust cloud is identified with the edge of the space-charge sheath. The formation of the central void was seen in many similar investigations, e.g., in Refs. [15–17], and is explained by a force balance between the ion-drag force from the ambipolar ion flow out of the plasma center and the ambipolar electric field force [18].

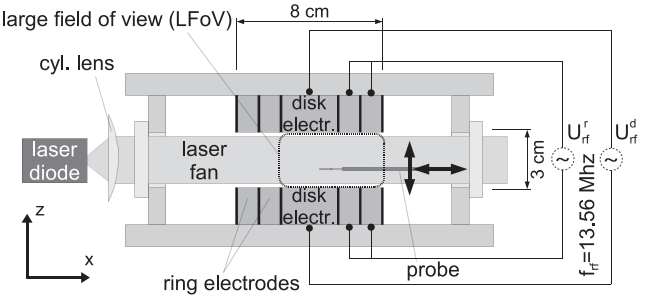

FIG. 1. Side view of the IMPF-K device. The rf discharge has segmented electrodes and is operated in push-pull mode between pairs of electrodes. The two ring electrodes are electrically connected.

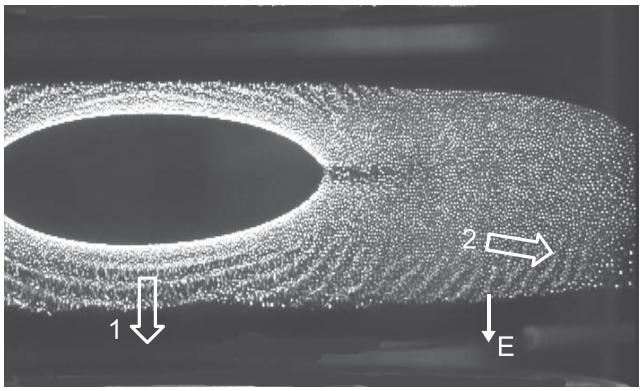

FIG. 2. Still image of dust-density waves. The framed arrows indicate the wave propagation direction. The arrow in region 1 indicates the ordinary DDW and the arrow in region 2 the OPDDW. The electric field direction is perpendicular to the sheath boundary. The electric field E near the electrode sheath is perpendicular to the boundary of the dust cloud. The dust cloud shows a weak top-bottom asymmetry, which is caused by residual gravity.

The waves are seen as a strong spatial modulation of the dust density. Close to the void edge, the wave fronts (visible as bright wave crests) move vertically away from the void (arrow 1) with a velocity of $v_{\mathrm{DDW}} = 16.8\ \mathrm{mm\,s^{-1}}$. Further away from the void, the wave fronts change their orientation and finally become strongly inclined with respect to the sheath edge (arrow 2). This behavior was not expected for the ordinary DAW, because the ion flow that excites the unstable DDW is aligned with the electric field. Since this electric field is also responsible for the force equilibrium of the dust particles at the edge of the dust cloud, the electric field must be strictly perpendicular to the dust boundary. Otherwise, a dust flow along the boundary would be observed. We call this unusual wave an "obliquely propagating dust-density wave" (OPDDW).

The frequency of the OPDDW is $f_{\mathrm{OP}} = 11$ Hz, and the propagation velocity, as obtained from the displacement of the wave fronts in subsequent frames, is $v_{\mathrm{OP}} = 16\ \mathrm{mm\,s^{-1}}$. This propagation velocity is similar to v_{DDW} found at the void edge. The phase fronts are found to have an inclination of $\theta = 40°$–$60°$ with respect to the sheath boundary. The mean wavelength is $\lambda = 1.5 \pm 0.15$ mm.

Model for the OPDDW.—The DDW is described by the electrostatic dispersion relation [19]

$$0 = 1 + \chi_e + \chi_i + \chi_d, \tag{1}$$

which contains the susceptibility of the electrons $\chi_e = (k\lambda_{\mathrm{De}})^{-2}$, where k is the wave number and $\lambda_{\mathrm{De}} = [\epsilon_0 k_B T_e/(n_e e^2)]^{1/2}$ the electron Debye length. The susceptibility of the dust

$$\chi_d = -\frac{\omega_{\mathrm{pd}}^2}{\omega(\omega + i\nu_{\mathrm{dn}})} \tag{2}$$

depends on the dust plasma frequency $\omega_{\mathrm{pd}} = [Z_d^2 e^2 n_d/(\epsilon_0 m_d)]^{1/2}$ (Z_d, n_d, m_d being the dust charge number, density, and mass), the wave frequency ω and the dust-neutral collision frequency ν_{dn}.

The ion susceptibility is derived from a fluid model that includes a streaming velocity v_0 in z direction, a thermal velocity $v_{\mathrm{Ti}} = (k_B T_i/m_i)^{1/2}$, and a collision frequency ν, which accounts for ion collisions with neutrals and with dust particles. Assuming all wave quantities (density $\tilde{n}$, velocity $\tilde{v}$, potential $\tilde{\phi}$) to vary as $\exp[i(k_x x + k_z z - \omega t)]$ the ion equation of motion becomes

$$\begin{aligned} -i\Omega_1 n_{i0} m_i \tilde{v}_x &= -ik_x n_{i0} e\tilde{\phi} - ik_x k_B T_i \tilde{n}_i, \\ -i\Omega_2 n_{i0} m_i \tilde{v}_z &= -ik_z n_{i0} e\tilde{\phi} - ik_z k_B T_i \tilde{n}_i, \end{aligned} \tag{3}$$

where n_{i0} is the equilibrium ion density and the coordinates are chosen such that the z direction is defined by the ion flow. $\Omega_1 = \omega + i\nu$, $\Omega_2 = \omega + i\nu - k_z v_0$. Note that Ω_2 is markedly different from Ω_1 because of the Doppler shift. This implies that the ion oscillation velocity $(\tilde{v}_x, \tilde{v}_z)$ is not aligned with the wave vector (k_x, k_z). The magnetic field associated with the transverse part of the ion current can be neglected because of the low frequencies involved. Inserting the oscillation velocities from Eq. (3) into the linearized equation of continuity

$$-i\Omega_3 \tilde{n}_i + i(k_x \tilde{v}_x + k_z \tilde{v}_z) n_{i0} = 0, \tag{4}$$

we obtain the relationship between $\tilde{n}_i$ and $\tilde{\phi}$. Here $\Omega_3 = \omega - k_z v_0$ also includes the Doppler shift. Finally, we obtain the ion susceptibility $\chi_i = -(e\tilde{n}_i)/(\epsilon_0 k^2 \tilde{\phi})$ as a function of the orientation angle $\theta = \arccos(k_z/k)$ between k and ion beam direction z

$$\chi_i = \frac{-\omega_{\mathrm{pi}}^2}{\Omega_1 \Omega_2 \Omega_3 \Omega_4^{-1} - k^2 v_{\mathrm{Ti}}^2} \tag{5}$$

with the abbreviation $\Omega_4 = \Omega_1 \cos^2\theta + \Omega_2 \sin^2\theta$. Our result is more general than the fluid limit discussed in Ref. [8], which we would obtain by imposing the additional requirement that the oscillation velocity becomes strictly aligned with the wave vector.

Equation (5) gives the well-known limiting cases, (a) for stationary warm and collisionless ions: $\chi_i \approx (k\lambda_{\mathrm{Di}})^{-2}$ with the ion Debye length $\lambda_{\mathrm{Di}} = v_{\mathrm{Ti}}/\omega_{\mathrm{pi}}$, and (b) for stationary cold ions: $\chi_i \approx -\omega_{\mathrm{pd}}^2/\omega(\omega + i\nu)$.

A simplified limiting case for χ_i in the presence of drifting ions is found for large propagation angles, where $\sin^2\theta \approx 1$ and $\Omega_4 \approx \Omega_2$. Neglecting ω in Ω_1 and Ω_3, which is justified for the typical beam velocities and ion collision frequencies of the experiment, and dropping $k^2 V_{\mathrm{Ti}}^2$ as small, we obtain the purely imaginary value

$$\chi_i \approx \frac{\omega_{\mathrm{pi}}^2}{i\nu k v_0 \cos\theta}. \tag{6}$$

Here, $|\chi_i|$ increases when v_0 is lowered or when $\theta \to 90°$.

In the limit $\theta = 0°$ the condition $\Omega_4 = \Omega_1$ holds which, with the same simplifications as above, leads to

$$\chi_i \approx \frac{\omega_{\mathrm{pi}}^2}{k v_0 (i\nu - k v_0)}. \quad (7)$$

This time, when v_0 is lowered, $|\chi_i|$ increases approximately with $(k v_0)^{-2}$ and is therefore very sensitive to changes in the ion velocity.

Since the wave frequency ω can be neglected in χ_i compared to the ion collision frequency, the dispersion relation Eq. (1) becomes

$$\omega = -\frac{i}{2}\nu_{\mathrm{dn}} + \left(-\frac{1}{4}\nu_{\mathrm{dn}}^2 + \frac{\omega_{\mathrm{pd}}^2}{1 + \chi_e + \chi_i}\right)^{1/2}. \quad (8)$$

Comparison with experiment.—The dispersion relation is calculated for typical experimental parameters, ion density $n_{i0} = 3 \times 10^{14}$ m^{-3}, electron temperature $T_e = 2.5$ eV, and dust density $n_{d0} = 5 \times 10^{10}$ m^{-3}. The dust charge was assumed as $Z_d = 4000$ according to recent experiments [20], which result in values much lower than the expectation from the classical OML model ($Z_d^{\mathrm{OML}} = 9900$). The ion-neutral collision frequency was chosen as $\nu_{\mathrm{in}} = v_0/\lambda$ with $\lambda(\mathrm{m}) = 3.28 \times 10^{-3}/p(\mathrm{Pa})$ [21]. Ion-dust collisions, which are less frequent [22], are also included. As discussed in Ref. [16], we have chosen the drift velocity close to the sheath edge as the Bohm velocity $v_B = (k_B T_e/m_i)^{1/2}$. The situation in the interior of the dust cloud is modeled by choosing a smaller value of the ion drift velocity ($v_0 = 0.3 v_B$). The resulting real and imaginary part of ω as a function of the real wave number k at these standard conditions are shown in Fig. 3(a) and 3(b) for propagation angles 0°, 45°, 70°, and 80°.

The dispersion relation $\mathrm{Re}\{\omega(k)\}$ at 0° shows an increase of the frequency with wave number, which is asymptotically linear at small wave numbers and approaches the dust plasma frequency ($\omega_{\mathrm{pd}} = 96$ s^{-1}) at large wave numbers. In this way it resembles the shape of dust-acoustic dispersion. For increasing propagation angle θ the initial slope of the curve decreases, indicating a reduction in phase velocity. The experimental result for the frequency and wave number of the beam driven OPDDW is shown with error bars. The calculated dispersion curves approach the experimental situation with increasing angle of propagation, although no quantitative agreement is found. Better agreement would be obtained for a reduced value of the dust plasma frequency at the sheath edge. The wave damping can be read from the imaginary part $\mathrm{Im}\{\omega(k)\}$ in Fig. 3(b). Positive values indicate wave growth. The growth rate increases for larger propagation angles. The fastest growing mode, which finally determines the observed nonlinearly saturated wave in the experiment, is found at large propagation angles. Hence, the model explains the existence of an OPDDW mode that propagates at high inclination to the ion drift direction.

For comparison, we have recalculated the dispersion relation at $v_0 = 0.3 v_B$ [Fig. 3(c) and 3(d)]. Here, the waves propagating along the ion beam are most unstable. This result is consistent with the experimental finding that, inside the dust cloud, where the electric field is expected to have lower values, the wave initially propagates as a DDW in the direction of the electric field. Now the experimental point is found in better agreement with the dispersion relation for small propagation angles. Moreover, the experimental wave number is close to the maximum of the growth rate. This finding supports the correct choice of the

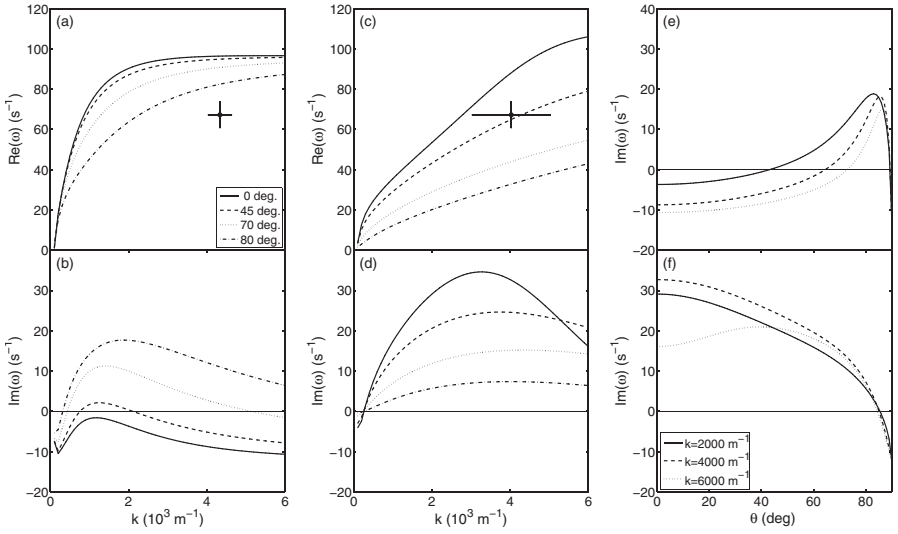

FIG. 3. (a) Real part of the wave frequency as a function of the wave number k for different orientation angles between wave propagation and ion beam. Ion velocity $v_0 = v_B$. The observed wave in region 2 is indicated with error bars. (b) Imaginary part of the wave frequency. Positive values indicate wave growth. (c), (d) Same as (a), (b), but at reduced ion velocity $v_0 = 0.3 v_B$. The experimental point is from region 1. (e) Growth rates for different wave numbers as a function of orientation angle at $v_0 = v_B$. (f) Same as (e), but for $v_0 = 0.3 v_B$.

parameters n_d and Z_d near the void, which determine the dust plasma frequency. In view of a decay of ion density towards the electrode sheath, it is reasonable to expect a related reduction of Z_d at the sheath edge. This would qualitatively explain the differences between experiment and theory in Fig. 3(a).

The dependence of the growth rate on the propagation angle for different values of the wave number k is compiled in Fig. 3(e) and 3(f) for ion drift at Bohm velocity and at reduced velocity showing the preference of the OPDDW at fast ion flows and the preference of the ordinary DDW at lower flow velocities.

Calculations at a reduced dust density of $n_d = 5 \times 10^9$ m^{-3} show that all modes become damped, which quenches the instability for all angles, confirming a critical dust density for the onset of strong DDWs. The wave dispersion and growth at an increased pressure of 50 Pa shows that all modes are damped. This demonstrates the observed quenching of the instability by gas friction, as found in Ref. [23].

Different from the unstable oblique DAW mode found in a collisionless magnetized plasma [24], which is excited by inverse ion Landau damping, the OPDDW invokes collisional ions ($\nu_i \gg \omega$) and the instability is of a resistive type. The observed preference for oblique propagation at high ion drift velocity can be understood as an increase of interaction time of the ion beam with the wave that compensates for the higher ion velocity. While the model of Mamun and Shukla [11] principally allows for oblique propagation of unstable DDWs, the authors did not discuss the case of wave propagation at large angles. Rather, for small drift velocities [$v_0 \cos\theta = (0.001 - 0.01) v_{\mathrm{Ti}}$], they find the most unstable mode for $\theta = 0°$, which agrees with the tendency reported here for small drift velocities. Rosenberg's model [8] deserves credit to contain the first theoretical prediction of unstable oblique dust-density waves. Our analysis goes beyond that model in that the critical dependence of the preferred propagation direction on the ion velocity was recognized. In summary, the OPDDW found in our experiments can be considered as a new observation in dusty plasmas which demonstrates that an electrostatic wave is not necessarily a one-dimensional phenomenon.

This work is supported by DLR under Contracts No. 50WM0338/50WM0339 and in parts by No. DFG-TR24/A2. The expert assistance by Mattias Kroll, Michael Poser, and Volker Rohwer is gratefully acknowledged.

*Electronic address: piel@physik.uni-kiel.de

[1] A. Barkan, R. L. Merlino, and N. D'Angelo, Phys. Plasmas **2**, 3563 (1995).
[2] C. Thompson, A. Barkan, N. D'Angelo, and R. L. Merlino, Phys. Plasmas **4**, 2331 (1997).
[3] V. I. Molotkov, A. P. Nefedov, V. M. Torchinskii, V. E. Fortov, and A. G. Khrapak, JETP **89**, 477 (1999).
[4] E. Thomas, Jr. and R. L. Merlino, IEEE Trans. Plasma Sci. **29**, 152 (2001).
[5] S. Ratynskaia, S. Khrapak, and A. Zobnin *et al.*, Phys. Rev. Lett. **93**, 085001 (2004).
[6] T. Trottenberg, D. Block, and A. Piel, Phys. Plasmas **13**, 042105 (2006).
[7] N. N. Rao, P. K. Shukla, and M. Y. Yu, Planet. Space Sci. **38**, 543 (1990).
[8] M. Rosenberg, J. Vac. Sci. Technol. A **14**, 631 (1996).
[9] N. D'Angelo and R. L. Merlino, Planet. Space Sci. **44**, 1593 (1996).
[10] P. Kaw and R. Singh, Phys. Rev. Lett. **79**, 423 (1997).
[11] A. A. Mamun and P. K. Shukla, Phys. Plasmas **7**, 4412 (2000).
[12] M. Rosenberg, J. Plasma Phys. **67**, 235 (2002).
[13] R. Bharuthram and S. V. Singh, Phys. Scr. **55**, 345 (1997).
[14] M. Klindworth, O. Arp, and A. Piel, J. Phys. D: Appl. Phys. **39**, 1095 (2006).
[15] G. E. Morfill, H. M. Thomas, and U. Konopka *et al.*, Phys. Rev. Lett. **83**, 1598 (1999).
[16] M. Klindworth, A. Piel, and A. Melzer *et al.*, Phys. Rev. Lett. **93**, 195002 (2004).
[17] G. Praburam and J. Goree, Plasma Sources Sci. Technol. **5**, 84 (1996).
[18] J. Goree, G. E. Morfill, V. N. Tsytovich, and S. V. Vladimirov, Phys. Rev. E **59**, 7055 (1999).
[19] P. K. Shukla and M. M. Mamun, *Introduction to Dusty Plasma Physics* (IOP, Bristol, 2002).
[20] S. A. Khrapak, S. V. Ratynskaia, and A. V. Zobnin *et al.*, Phys. Rev. E **72**, 016406 (2005).
[21] L. S. Frost, Phys. Rev. **105**, 354 (1957).
[22] S. A. Khrapak, A. Ivlev, S. K. Zhdanov, and G. E. Morfill, Phys. Plasmas **12**, 042308 (2005).
[23] S. Ratynskaia, M. Kretschmer, and S. Khrapak *et al.*, IEEE Trans. Plasma Sci. **32**, 613 (2004).
[24] R. Bharuthram and P. K. Shukla, Planet. Space Sci. **40**, 973 (1992).